

# A Study of Aluminum-Substituted Iron Dextran Complexes by Mössbauer Spectroscopy and X-ray Diffraction

Tianrong Cheng,<sup>†</sup> Robert Bereman,<sup>\*,†</sup> Eddy De Grave,<sup>‡,§</sup> and Larry H. Bowen<sup>†,||</sup>

Department of Chemistry, North Carolina State University, Box 8204, Raleigh, North Carolina 27695-8204, and Department of Subatomic and Radiation Physics, University of Ghent, B-9000 Ghent, Belgium

Received June 15, 2000. Revised Manuscript Received October 11, 2000

Two aluminum-substituted iron dextran complexes and one nonsubstituted have been synthesized and characterized by Mössbauer spectroscopy over a wide temperature range (10–298 K) and by X-ray powder diffraction at room temperature. The mean coherence lengths in the directions perpendicular to (211) and (200) are different, indicating that the core iron oxide materials are oblong in shape. The X-ray diffraction patterns of all complexes are very similar, with broad, weak peaks at 5.0, 3.3, 2.5, 2.25, 1.6, and 1.8 Å. These values are consistent with cell-contracted akaganeite,  $\beta$ -FeOOH. The three samples exhibit different temperatures for the onset of magnetic splitting in their Mössbauer spectra. The Mössbauer spectra obtained at room temperature can be adequately fitted with a model-independent distribution of quadrupole doublets, while at low temperatures a superposition of distributions of sextets and doublets is required. The obtained Mössbauer parameters are in line with the structural features. This is the first report on nanoscale aluminum-substituted iron oxides as a component of iron dextran.

## 1. Introduction

There is an increasing interest in the science community for nanoscale systems such as carbon-based nanotubes, nanocomposites, and small-particle magnetic systems. Water-soluble complexes, with iron cores in the nanoscale region, have so far not been studied as potential precursors to new electronic or catalytic materials. It has been known for quite some time that polyols and polysaccharides can stabilize nanoscale iron(III) oxides as colloidal materials at a pH near 7.<sup>1</sup> Examples of the systems that have been studied include fructose,<sup>2</sup> citrate,<sup>3</sup> sorbitol,<sup>4</sup> and various sugars.<sup>5</sup> Dextran is one of the polysaccharides that have been used extensively in our laboratory. Our previous work<sup>6–10</sup> with polysaccharide iron-oxide complexes, which are currently

utilized as sources for both oral iron therapy and injectable iron therapy, has demonstrated that the oxide cores in dextran complexes are in a cell-contracted akaganeite ( $\beta$ -FeOOH) phase and that these cores are around 4 nm in diameter.

We have undertaken a study of iron dextrans that are doped with various metals with the goal of developing alternative safe delivery agents. With the many other metals essential for a healthy human such as magnesium, zinc, selenium, copper, manganese, chromium, and molybdenum, our study has focused initially on Al-substituted complexes. In addition, in the field of clay and soil science, structures and magnetic properties of aluminum-substituted iron(III) oxides are major research objectives. And finally, with the search for new nanoscale materials and catalysts, developing efficient methods to “load” solubilized iron oxides becomes of interest.

Aluminum-substituted iron(III) oxides with different structure phases, such as substituted hematites,<sup>11–14</sup> maghemites,<sup>15–17</sup> goethites,<sup>18</sup> and ferrihydrites<sup>19,20</sup> have

\* To whom correspondence should be addressed.

<sup>†</sup> North Carolina State University.

<sup>‡</sup> University of Ghent.

<sup>§</sup> Research Director, Fund for Scientific Research–Flanders.

<sup>||</sup> Deceased. Professor Larry Bowen was a leader in these studies of Al-substituted iron oxides and his early advice and help will always have a positive impact on our work.

(1) Barker, S. A.; Somers, P. J.; Stevenson, J. *Carbohydr. Res.* **1974**, *36*, 331.

(2) Charley, P. J.; Sarkar, B.; Stitt, C. F.; Saltman, P. *Biochim. Biophys. Acta* **1963**, *69*, 313.

(3) Spiro, T. G.; Pape, L.; Saltman, P. *J. Am. Chem. Soc.* **1967**, *89*, 5555.

(4) Tonkovic, M.; Hadzija, O.; Nagy-Czako, I. *Inorg. Chim. Acta* **1983**, *80*, 251.

(5) Nagy, L.; Burger, K.; Kurti, J.; Mostafa, M. A.; Korecz, L.; Kiricsi, I. *Inorg. Chim. Acta* **1986**, *124*, 55.

(6) Knight, B.; Bowen, L. H.; Bereman, R. D.; Huang, S.; De Grave, E. *J. Inorg. Biochem.* **1999**, *73*, 227–233.

(7) Coe, E. M.; Bowen, L. H.; Bereman, R. D.; Speer, J. A.; Monte, W. T.; Scaggs, L. *J. Inorg. Biochem.* **1995**, *57*, 63–71.

(8) Coe, E. M.; Bowen, L. H.; Speer, J. A.; Wang, Z.; Sayers, D. E.; Bereman, R. D. *J. Inorg. Biochem.* **1995**, *34*, 269–278.

(9) Coe, E. M.; Bowen, L. H.; Speer, J. A.; Bereman, R. D. *J. Inorg. Biochem.* **1995**, *57*, 287–292.

(10) Coe, E. M.; Bowen, L. H.; Bereman, R. D.; Monte, W. T. *Inorg. Chim. Acta* **1994**, *223*, 9–14.

(11) Srivastava, J. K.; Sharma, R. P. *Phys. Status Solidi B* **1972**, *49*, 135.

(12) Kren, E.; Molnar, B.; Svab, E.; Zsoldos, E. *Solid State Commun.* **1974**, *15*, 1707.

(13) Murad, E.; Schwertmann, U. *Clays Clay Miner.* **1986**, *34*, 1–6.

(14) DeGrave, E.; Bowen, L. H.; Weed, S. B. *J. Magn. Magn. Mater.* **1982**, *27*, 98.

(15) Bowen, L. H.; De Grave, E.; Bryan, A. M. *Hyperfine Interactions* **1994**, *94*, 1977–1982.

(16) Da Costa, G. M.; De Grave, E.; Bowen, L. H.; De Bakker, P. M. A.; Vandenbergh, R. E. *Phys. Chem. Miner.* **1995**, *22*, 178–185.

been reported. However, to the best of our knowledge, aluminum-substituted iron(III) oxides with an akaganeite structure phase has not been reported. In addition, no metal-substituted iron dextrans have been reported. Taking the above factors into consideration, three aluminum-substituted iron(III) oxide dextrans have been prepared in our lab.

Our previous work with polysaccharide iron-oxide complexes has applied two particularly useful techniques: Mössbauer spectroscopy and powder X-ray diffraction. They probe the solid-state structure in the iron oxide core, but not the dextran coating. Powder X-ray diffraction is sensitive to long-range crystalline order and thus allows the distinction between different mineralogical forms of iron oxide. In the case of nano-scale materials, there is considerable broadening of the diffraction lines that can make the determination of line positions, and hence phase identification, difficult. However, this broadening is directly related to the length of the diffracting zone and thus provides a measure of the size of the iron-oxide core. Mössbauer spectroscopy is complementary in that it is extremely sensitive and specific to the local environment around the probe Fe nuclei and to the magnetic state of the core, which is size dependent.

## 2. Experimental Section

**Synthesis.** Iron dextran (ID), designed to serve as a standard for the synthesis procedures for all other samples, was synthesized by mixing 12 mL of a 1.48 M FeCl<sub>3</sub> aqueous solution with 8 mL of a 1.1 M Na<sub>2</sub>CO<sub>3</sub> aqueous solution. To this rapidly stirred mixture, 14 mL of a solution containing 4.0 g of ≈6000 MW dextran was added. Subsequently, a 3.55 M solution of NaOH was added carefully to adjust the pH to between 9 and 10. The reaction mixture was then heated to 90 °C for 2 h and afterward cooled to room temperature (RT). To this solution was added 40 mL of 2-propanol, resulting in the formation of solid ID. The supernatant solution was removed and the solid was dissolved in 20 mL of water. The process of precipitation with 2-propanol and dissolving in water was repeated three times. The resulting solid was then air-dried overnight.

Two different samples of iron dextran with Al(III) substituted into the core were prepared. In the first procedure, sample IAD1, iron/aluminum oxide, was prepared with both iron and aluminum present at the beginning of the reaction. The synthetic process was the same as that of above except that the starting materials were 6 mL of 1.48 M ferric chloride, 3 mL of 1.48 M aluminum chloride, and 6 mL of 1.1 M sodium carbonate. The pH was adjusted to 9–10 by 3.55 M sodium hydroxide solution. The dextran solution was made from 3 g of dextran (≈6000 MW) in 10 mL of water. Thus, the reactant ratio is the same as that used for the ID synthesis.

The second iron/aluminum oxide (IAD2) was prepared by adding Al(III) at a later stage of the reaction. The goal was to produce a sample with a higher Al(III) concentration near the surface of the core material. The synthesis procedure was identical to that of ID and IAD1. The amount of starting materials were the same as those for IAD1 except that 3 mL (1.48 M) of aluminum chloride was added after 1 h of heating of the reaction mixture, instead of adding it at the same time as ferric chloride as in the case of IAD1.

**Table 1. Elementary Analysis Results**

sample	Fe %	Al %	Al/(Fe + Al) (mol)
ID	27.69	0	0
IAD1	17.74	3.41	0.284
IAD2	21.65	3.47	0.250

**Elemental Analysis.** Elemental analyses were obtained from Galbraith Laboratories, Knoxville, TN. The Fe and Al contents are summarized in Table 1.

**X-ray Powder Diffraction.** X-ray powder diffraction (XRD) patterns were obtained with a Rigaku D/Max-B series diffraction system equipped with a graphite monochromator and using Cu K $\alpha$  radiation. Scans were made from 10° to 70° (2 $\theta$ ) with a goniometer speed of 0.5°/min. The samples for the diffraction experiments were prepared by grinding the powders in acetone and allowing the resulting suspension to dry on an oriented quartz plate to decrease the background. The quartz (211) reflection was used as an internal standard both for the correction of the peak positions and for the estimation of the contribution of instrumental line broadening to the observed width of the sample peaks. The mean coherence lengths (MCL) of the iron-oxide cores were obtained from the well-known Scherrer approximation<sup>21</sup> assuming  $K = 0.9$ .

**Mössbauer Spectroscopy.** Mössbauer spectra (MS) were obtained with the respective absorbers kept at temperatures of 12, 15, 20, 25, 30, 35, 40, 45, 50, 60, 70, and 298 K (RT) using a closed-cycle helium cryostat maintained at the required setpoint to within about 0.1 K. The spectrometer was an Austin Science Associate's constant-acceleration drive with a sawtooth reference signal. The velocity scale was calibrated after each run using a He/Ne laser interferometer. Data were collected in 512 channels. The <sup>57</sup>Co(Rh) source, with an initial activity of 50 mCi, was kept at RT. Absorbers that consisted of mixtures of the Fe/Al dextran samples and powdered sucrose were pressed flat into a uniform thickness of ≈10 mg of Fe/cm<sup>2</sup> and sealed in brass rings with an aluminum-foil backing.

The MS were fitted after subtraction of the signal due to Fe impurities in the cryostat windows and in the aluminum backing. A model-independent distribution of doublets at RT and a superposition of distributed doublets and sextets at low temperatures were found to produce excellent reproductions of the MS.<sup>22</sup> The elementary line shape was assumed to be Lorentzian. For the sextet components the outer-line to inner-line area ratio was fixed at 3 and for the middle-line to inner-line ratio at 2. The center shift  $\delta$  and the quadrupole shift  $\Delta E_Q$  were allowed to vary. Symmetrical doublets were used for the paramagnetic contributions, with  $\delta$  and the quadrupole splitting  $\Delta E_Q$  adjustable parameters. In cases where both a doublet and sextet coexisted, the  $\delta$  values of the two components were set to be equal.

## 3. Results and Discussion

**X-ray Powder Diffraction.** The XRD patterns of the three samples are reproduced in Figure 1. Several broad peaks are obvious; the most prominent one corresponds to a lattice spacing  $d \approx 2.5$  Å, which is, however, common for various iron (oxyhydr) oxides. Also characteristic of iron oxides are the peaks at ≈1.5 and at ≈5.0 Å. Comparison of the respective  $d$  values with data reported for iron (oxyhydr) oxides and iron-oxide cores<sup>7</sup> suggests that the major constituent in these samples is most likely a cell-contracted akaganeite,  $\beta$ -FeOOH.<sup>8,23</sup> The XRD patterns of this phase and of the present samples do not match closely with those of "normal", relatively well-crystallized akaganeite<sup>24,25</sup> because a major peak at 7.41 Å is absent in the cell-contracted

(17) Amarasiriwardena, D. D.; De Grave, E.; Bowen, L. H. *Clays Clay Miner.* **1986**, *34*, 250–256.

(18) Schwertmann, U.; Murad, E. *Clays Clay Miner.* **1983**, *31*, 277–284.

(19) Chadwick, J. C.; Jones, D. H.; Thomas, M. F.; Devenish, M. *Hyperfine Interact.* **1986**, *28*, 537–540.

(20) Chadwick, J. C.; Jones, D. H.; Thomas, M. F.; Tatlock, C. J.; Devenish, M. *J. Magn. Magn. Mater.* **1986**, *61*, 88–100.

(21) Klug, H. P.; Alexander, E. *X-ray Diffraction Procedures for Polycrystalline and Amorphous Materials*; Wiley: New York, 1974.

(22) Amarasiriwardena, D. D.; Bowen, L. H.; Weed, S. B. *Soil Sci. Soc. Am. J.* **1988**, *52*, 1179.

(23) Chandry, K. C. *Mineral. Mag.* **1965**, *35*, 666.

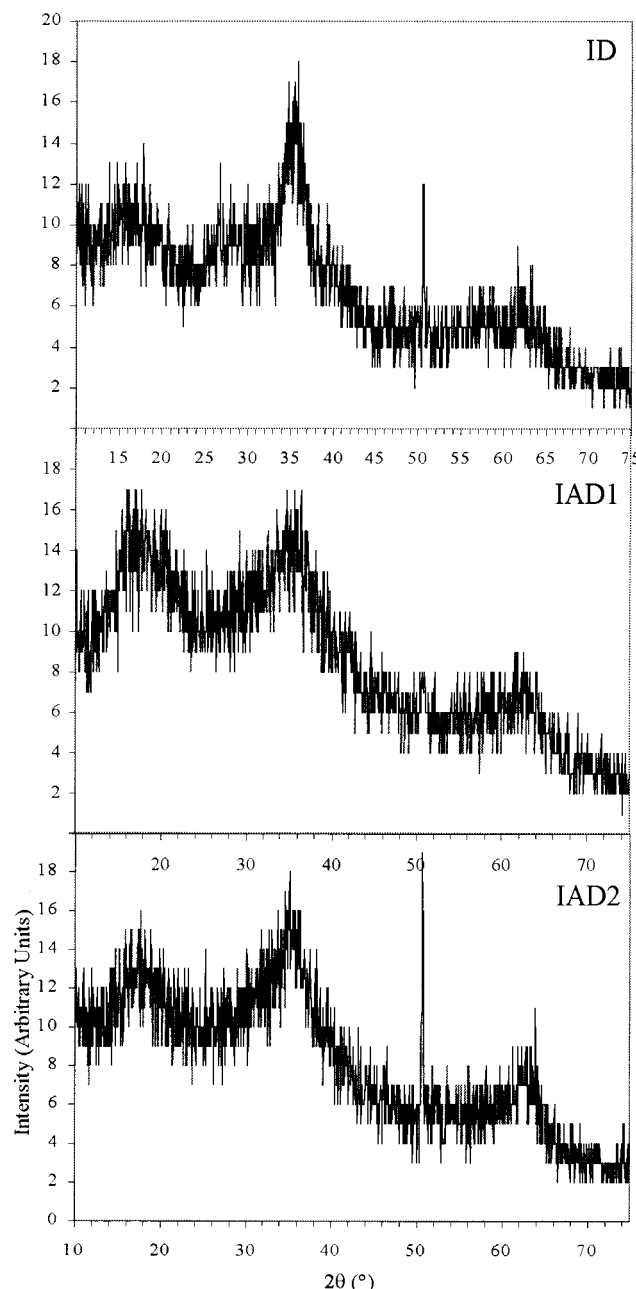


**Figure 1.** XRD patterns of ID, IAD1, and IAD2.

form and other peaks are markedly shifted to different diffraction angles.<sup>7,23</sup> Considering the synthesis conditions, more specifically the presence of chlorine species in the parent solution, the formation of  $\beta$ -FeOOH is not surprising.<sup>26</sup>

Curve fitting (mixed Gauss and Lorentzian) was used to precisely quantify positions and line widths of the prominent diffraction lines, that is, the (211) at  $2\theta \approx 35^\circ$  and the (200) at  $2\theta \approx 17^\circ$ . After correction based on the (211) line of the quartz sample holder (see section 2), the respective  $MCL_{211}$  and  $MCL_{200}$  were obtained following the procedure described.<sup>21</sup> The results are listed in Table 2. The data show that sample ID has the largest particle size and IAD1 the smallest. Because

**Table 2. Mean Coherence Length (MCL) Perpendicular to the Planes for the Two Most Prominent X-ray Diffraction Peaks:  $d(211) \sim 0.25$  nm;  $d(200) \sim 0.5$  nm**

sample	MCL(211) (nm)	MCL(200) (nm)
ID	3.1	1.60
IAD1	1.85	1.24
IAD2	2.02	1.56

the MCLs are different in each sample for different crystal planes, we conclude that the particles are nonspherical. They likely exhibit an elongated spindle shape<sup>27</sup> as has been observed in some other iron dextran samples.

It is surprising that there exists a dependence of the core size and the relative Al content, on one hand, and the method of synthesis, on the other hand. First, the amount of Al incorporation is clearly affected by the synthesis procedure. The simultaneous addition of  $AlCl_3$  and  $FeCl_3$  (sample IAD1) seems to result in a lower iron content in the core as compared to the delayed addition of  $AlCl_3$  (sample IAD2). It is expected that in this latter case the Al is also less uniformly distributed throughout the core than when the reagents are used together. In general, the particle size is smaller in the Al-substituted samples than in the Al-free sample. In addition, it appears that a trend exists that a higher Al mole ratio,  $Al/(Al + Fe)$ , leads to a smaller core size. A linear regression between this ratio and  $MCL_{211}$  yields  $MCL_{211} = 3.10 - 4.37 Al/(Al + Fe)$ , with  $R^2 = 0.9997$ . Initially, it was considered that the variations are a result of the lower coordination ability of Al(III), as compared to Fe(III), at the surface. However, Schulze and Schwertmann,<sup>28</sup> Da Costa et al.,<sup>29</sup> and De Grave et al.<sup>14,30</sup> have reported a similar result for aluminous goethite, maghemite, and hematite samples, respectively. They suggested that the change might be associated with the rate of crystal growth, which decreases as Al in the system rises.

**Mössbauer Spectra.** Some typical MS are shown in Figure 2. Mössbauer data at three different temperatures (the lowest applied temperatures, 70 K and room temperature 298 K) are shown in Table 3. At all temperatures the values obtained for the isomer shift  $\delta$  indicate the presence of high-spin Fe(III). The lowering of  $\delta$  with temperature in the range from 70 K to RT is plausible and is due to the second-order Doppler shift.<sup>31</sup> The MS at RT are nearly identical for the three samples and exhibit a pure doublet structure, indicating that none are magnetically ordered at RT. For each of these spectra a distribution of doublets was fitted to the data, with  $\Delta E_Q$  ranging from 0.2 to 1.5 mm/s. The isomer shifts of all three samples are identical, as expected for Fe(III) oxide samples, and also the maximum-probability and average  $\Delta E_Q$  values of the quadrupole-splitting distribution profiles are virtually the same, indicating that the distribution of the sizes of the iron cores in the three samples are similar.

(27) Voznyuk, P. O.; Dubinin, V. N.; Razumov, O. N. *Sov. Phys. Solid State* **1977**, *19*, 1884–1887.

(28) Schulze, D. G.; Schwertmann, U. *Clay Miner.* **1987**, *22*, 83–92.

(29) Da Costa, G. M.; Laurent, Ch.; De Grave, E.; Vandenberghe, R. E. *Mineral Spectroscopy: A Tribute to Roger G. Burns. The Geochemical Society, Special Publication* **1996**, No. 5, 93–104.

(30) De Grave, E.; Bowen, L. H.; Vochten, R.; Vandenberghe, R. E. *ibid* **1988**, *72*, 141.

(31) De Grave, E.; Alboom, V. *Phys. Chem. Miner.* **1991**, *18*, 337.

(24) Murad, E. *Clay Miner.* **1979**, *14*, 273.

(25) JCPDS Card, No. 13-157.

(26) Chambaere, D. G.; De Grave, E. *Phys. Status Solidi(a)* **1984**, *83*, 93–102.

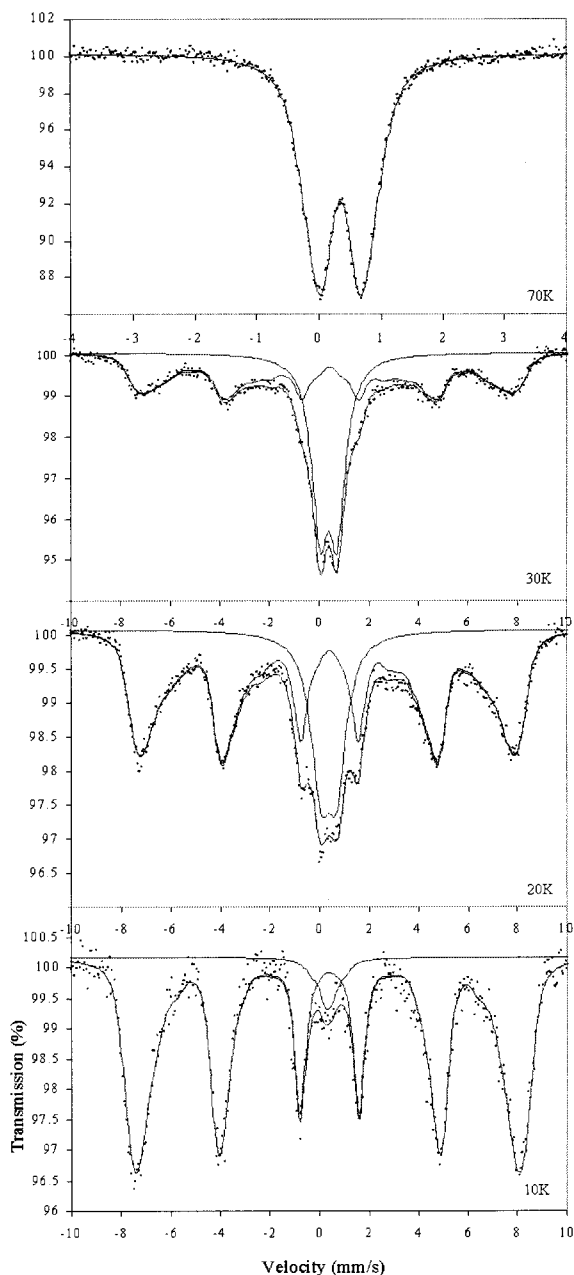


**Figure 2.** Typical Mössbauer spectra at different temperatures of all three samples. The spectra shown above are of sample ID.

For the low-temperature MS in which a sextet and a doublet component coexist, the magnetic hyperfine field,  $H_{\text{hf}}$ , was allowed to vary in the range of 120–540, while the distribution for  $\Delta E_{\text{Q}}$  was the same as that for the pure doublets at higher temperatures. An important datum is the doublet/sextet partition that is obtained from the relative spectral areas of the two components. The variations of this parameter with temperature are depicted for the three samples in Figure 3. From these curves the values of the parameters  $T_{1/2}$ , the temperature where the sextet and doublet contribute in a 50/50 ratio, and  $T_{\text{B}}$ , the temperature where the sextet completely collapses to a doublet, can be determined. The latter temperature is often referred to as the blocking temperature.<sup>6</sup> The values of  $T_{1/2}$  are found to be 33, 20, and 14 K for ID, IAD2, and IAD1, respectively, and those of  $T_{\text{B}} \approx 55, 35, \text{ and } 25 \text{ K}$ . Further, the temperature

**Table 3. Mössbauer Data at Different Temperatures**

$T$ (K)	% S, % D	I.S. (mm/s) <sup>a</sup>	Q.S. (mm/s) <sup>b</sup> mean/max.	field (kOe) mean/max.
ID				
10	96% S 4% D	0.47	-0.040	456/481
70	100% D	0.47	0.72/0.25	
298	100% D	0.45	0.76/0.57	
298	100% D	0.35	0.73/0.69	
IAD1				
7	82% S 18% D	0.45	-0.056	405/472
70	100% D	0.45	0.70/0.46	
298	100% D	0.45	0.78/0.80	
298	100% D	0.34	0.74/0.66	
IAD2				
9	88% S 12% D	0.45	-0.045	443/486
70	100% D	0.45	0.73/0.42	
298	100% D	0.45	0.74/0.66	
298	100% D	0.34	0.72/0.66	

<sup>a</sup> I.S.: isomer shift relative to iron metal. <sup>b</sup> Q.S.: quadrupole splitting.

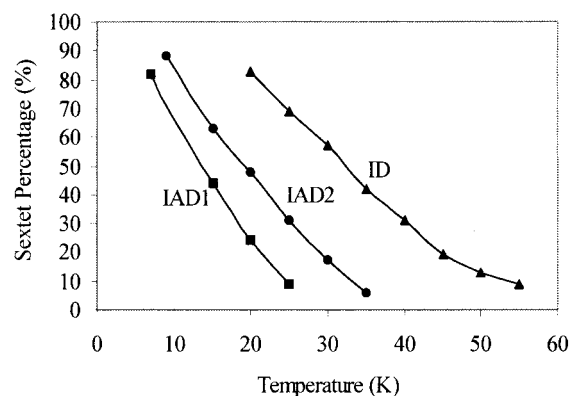


**Figure 3.** Variations of sextet % with temperature.

ranges at which a sextet and doublet coexist are 10–56 K ( $\Delta T = 46 \text{ K}$ ) for ID,  $\approx 4$ –36 K ( $\Delta T = 32 \text{ K}$ ) for IAD2, and  $\approx 2$ –26 K ( $\Delta T = 24 \text{ K}$ ) for IAD1.

A few major conclusions are inferred from these data. First, the iron dextran complex without Al (larger MCLs) has higher  $T_{1/2}$  and  $T_{\text{B}}$  “transition” temperatures than the complex containing Al in the iron cores (smaller MCLs). In addition, the sample with less Al in the iron cores has higher transition temperatures than that with a higher percentage of Al present. These two points coincide well with the particle-size and Al-for-Fe substitution effects observed for various iron oxides.<sup>14,28–30</sup> Finally, the  $\Delta T$  data suggest that the cores in sample IAD1 are more uniform in size than those in sample IAD2 and that ID is the least uniform among the three in that respect.

Data show that both the maximum-probability hyperfine fields,  $H_{\text{hf,m}}$ , and average hyperfine fields,  $H_{\text{hf,a}}$ , at the lowest applied temperatures are significantly lower for IAD1, on one hand, and ID and IAD2, on the other hand (Table 3). The low field values for IAD1 as compared to those for ID may be attributed to the effects of Al-for-Fe substitution. Because Al is diamagnetic, it does not contribute to the magnitude of the magnetic hyperfine field and its presence reduces the average number of Fe–O–Fe magnetic exchange paths, and hence the supertransferred hyperfine fields.<sup>14</sup> Further, the significantly smaller core size for IAD1 may also play an important role in the observed hyperfine-field differences.<sup>32</sup>

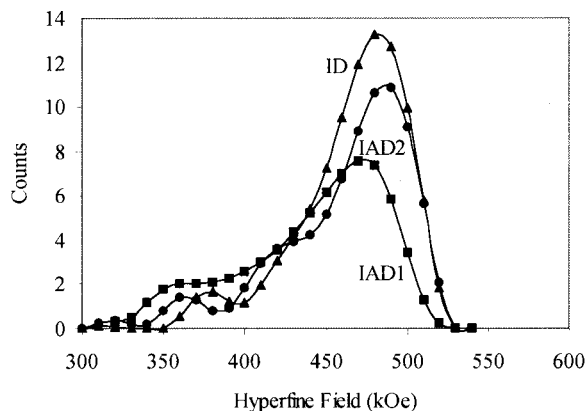


**Figure 4.** Hyperfine field distribution of samples ID ( $\blacktriangle$ , 10 K), IAD1 ( $\blacksquare$ , 7 K), and IAD2 ( $\bullet$ , 9 K).

The differences between the maximum probability hyperfine-field values for ID and IAD2 are less significant (Table 3). This finding suggests that the structure of at least a portion of the cores of both ID and IAD2 is similar. That is Al is believed to be distributed in the outermost layers of the iron-oxide core in sample IAD2. This is what was anticipated by the approach of the synthesis method, that is, adding the aluminum chloride 1 h after the initial reaction with iron(III) chloride was started.

The relationship,  $H_{\text{obs}} = H_0 (1 - kT/2K_a V)$ , is often applied to interpret the behavior of the MS of nanoscale iron oxides.<sup>33-36</sup> In this expression  $H_0$  is the hyperfine field for bulk material,  $H_{\text{obs}}$  is the observed field for the nanophase,  $k$  is Boltzmann's constant,  $V$  is the particle volume,  $K_a$  is the effective magnetic anisotropy constant, and  $T$  is the temperature of the measurement. Using the values of  $H_{\text{hf,m}}$  obtained in this study at different temperatures, the  $H_0$  fields were calculated to be 490 kOe for both ID and IAD2 and 477 kOe for IAD1, indicating again that cores in samples ID and IAD2 are most likely to be of a similar structure and composition.

This conclusion is supported by the evaluated hyperfine-field distribution profile for IAD2 at 9 K (Figure 4). Clearly, a second component in addition to the principal component with a field of 486 kOe and centered at around 430 kOe is present in this profile. It is plausible to attribute this component to the highly Al-substituted iron-oxide surface layers. Although the hyperfine-field distribution profiles for the other two samples are not symmetric either, no apparent shoulders are observed, indicating that the hyperfine-field distributions are continuous and that there is no abrupt change between the center part of the cores and the surface layers. We plan to use this to probe the surface reactivity of various substituted ID materials.

(32) Cornell, R. M.; Schwertmann, U. *The Iron Oxides-Structure, Properties, Reactions, Occurrence and Uses*; VCH Verlagsgesellschaft/VCH Publishers: Weinheim/New York, 1996.

(33) Williams, J. M.; Danson, D. P.; Janot, C. *Phys. Med. Biol.* **1978**, *23*, 835.

(34) Morup, S.; Topsoe, H. *Appl. Phys.* **1976**, *11*, 63.

(35) Morup, S.; Topsoe, H.; Lipka, J. *J. Phys. Colloq.* **1976**, *37*, C6.

(36) Morup, S.; Topsoe, H.; Clausen, G. S. *Phys. Scr.* **1982**, *25*, 713.

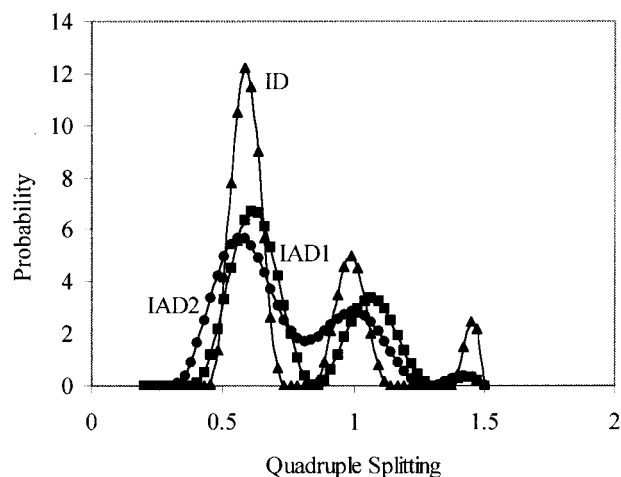


**Figure 5.** Quadrupole splitting distributions at  $T_B$  of sample ID ( $\blacktriangle$ ), IAD1 ( $\blacksquare$ ), and IAD2 ( $\bullet$ ).

Finally, at  $T_B$ , the quadrupole-distribution profiles for all three samples consist of two clearly resolved peaks (see Figure 5). At  $T_B$  their  $\Delta E_Q$  values are 0.6 and 1.0 mm/s for ID, 0.61 and 1.06 mm/s for IAD1, and 0.55 and 0.99 mm/s for IAD2. This finding strengthens the conclusion obtained from the XRD that all three samples have a core of akaganeite. Relatively well-crystallized  $\beta$ -FeOOH indeed has two distinct octahedral sites, which result in two quadrupole splittings, typically at 0.5 and 0.95.<sup>26</sup>

## Conclusions

It has been demonstrated in this work that Al-substituted iron dextrans can be prepared and that the core structure remains similar to that of cell-contracted akaganeite. The Al substitution has a significant effect on the size of the iron-oxide cores and hence on the magnetic hyperfine fields and relaxational behavior. We have seen that with an increasing percentage of Al, the iron oxide core sizes are smaller and the magnetic hyperfine fields of the cores are also smaller. We believe the size is related primarily to the crystal growth rate of cores. In addition, however, with fewer "coordination sites" for dextran at the surface, larger colloidal cores are not as stable. The diamagnetic property of Al lessens the magnetic contribution portion in the core and hence decreases the magnetic hyperfine field.<sup>32</sup> The quadrupole interactions are not affected by the Al content. It seems to be quite easy to prepare Al-substituted iron dextran samples with the Al distributed evenly throughout the core or localized in the surface layers. We are currently investigating addition metal-substituted iron dextrans.

**Acknowledgment.** Part of this work was performed in the framework of the Belgian "Interuniversity Attraction Poles" Program P4/10, granted by the Federal Office of Scientific, Technical and Cultural Affairs and of the NATO Collaborative Research Grant (#CRG. 960075).

CM000489V